Development of the Next Generation BACS Using AI and Human Factors

Kitoshi Tanaka*1 Takuro Kikuchi*2 Takeshi Takai*2 Takashi Kasuya*3

Summary

The spread of cloud computing and the Internet of Things (IoT), as well as the increase in computer resources such as GPUs, are expanding the possibilities for the application of Artificial Intelligence (AI). In this paper, we outline our AI-based human factor extraction, remote control of building equipment systems, and the data platform that enables them. As human factors, the authors used cameras to detect people and acquire the clothing insulation value. In addition, a reinforcement learning engine, which learns based on the building equipment and IoT data collected in the cloud, was applied to control lighting and air conditioning systems. Comparison of the system's actual data with simulations confirmed energy savings of more than 15% for lighting and 10% for air conditioning.

Keywords: cloud, human-factor, AI, IoT, building automation system

1 Introduction

The widespread adoption of cloud technologies, the Internet of Things (IoT) - which connects various devices to networks - and big data technologies that use statistical and machine learning techniques to extract insights from large amounts of data, have facilitated the establishment of an environment in which services related to advanced control and analysis can be offered at a low cost in a cloud environment. In building facilities, there is a growing demand for further advancements in energy-conservation technologies to achieve carbon neutrality. Furthermore, there is a need to enhance occupant comfort by capturing detailed environmental movements and reducing the workload through remote control and automation, given to the shortage of human resources for building management. To meet these needs, we propose a next-generation building equipment system that uses human factors and artificial intelligence to meet these needs. This study presents an overview of this system and the results of demonstration tests conducted at the Takenaka Research and Development Institute.

2 System overview

Fig. 1 depicts the developed system configuration, which consists of five components: (1) a group of building equipment systems; (2) a group of IoT sensors and systems that extract human factors; (3) a gateway; (4) a data platform (Takenaka Building Communication System); and (5) an AI learning engine for building control (reinforcement learning engine). The measured values and setting values from the first two components (component 1 and 2) are acquired at the granularity of approximately 1 min. These data are then sent to the data platform (component 4), which is built into the cloud via the gateway (component 3).

These data are referenced in real-time in the reinforcement learning engine (component 5), stored in the internal big data processing infrastructure, and provided for learning to the same component. The reinforcement learning conducted by component 5 performs learning based on stored data while attempting various controls based on real-time measured values and setting values. The control command from component 5 is transmitted to component 3 via the application programming interface (API) possessed by component 4, converted to the communication specifications of the on-site equipment, and transmitted to component 1 in real-time. For further details, please refer to Reference[1].

This system is operated at the Takenaka Research and Development Institute (Inzai City, Chiba Prefecture)[2]. The institute includes research, management, and experiment buildings with a total floor area of 39,150 m2 and approximately 200 researchers work there. In 2019, the building and facilities underwent renovation to create a space that enhances the creative ability of each

＊1 Chief Expert, Technology Producing, Technology Department
＊2 Chief Researcher, Research & Development Institute, PhD
＊3 Chief Engineer, ICT Engineering Division, PhD

individual, with the goal of improving their ability to create new value. In introducing the developed system, remote control points for heat source control were added, which were not included in the above-mentioned modifications. Additionally, cameras and gateways were installed to extract human factors. The following sections describe technologies that were used in the developed system to extract human factors, such as human position, pose, and insulation values, and demonstrate the system's AI-based control of building equipment through the results obtained.

3 Extraction of human factors

3.1 System overview

We developed a system that utilizes deep learning to detect people, estimate their positions, and estimate their insulation values based on images captured by multiple network cameras. Fig. 2 shows that the cameras were compact, ceiling-mounted models capable of capturing 360-degree images, which allowed for a wide range of coverage with minimal camera pressure. Existing trained models were utilized to efficiently develop the system. However, these models were trained using images captured with a perspective projection lens (so-called "ordinary" camera lens), resulting in significantly reduced inference accuracy when analyzing distorted fish-eye lens images. To address this issue we added a processing step in which the captured fish-eye image was expanded into multiple perspective projection images, inferences were made, and the results were integrated (Fig. 3). The system captured images at a frequency was every minute.

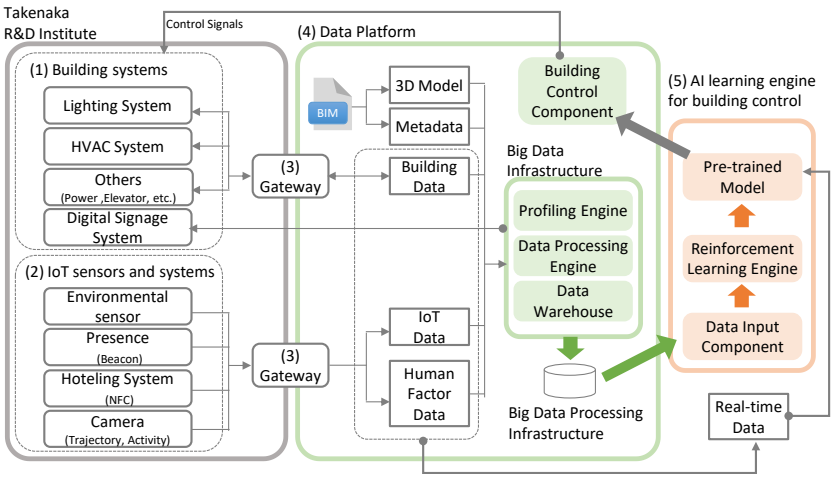

Fig.1 System configuration

3.2 Human detection, location, and insulation value estimation

A publicly available trained model (ssd_inception_v2_coco[3]) was used as the base model for human detection. To prepare a model for this study, a trained dataset was used for fine-tuning. An example of the training data is shown in Fig. 4, which consists of images of men and women in their 20s to 60s in postures and clothing commonly found in office environments. Each human region (whole body, upper body, lower body) and clothes were labeled with rectangles.

Fig. 2 Network camera

In addition, we introduced a pose estimation method that estimates the positions of various body parts, such as the head, shoulders, elbows, wrists, waist, knees, and ankles, for the rectangle obtained by the human detection. This allows for more accurate determination of the position of a person's feet more accurately and improves the accuracy of estimating a person's position in the original space. To achieve this, we utilized a pre-trained model (human-pose-estimation-0001[4]) for which the pose estimation had also published. Fig. 5 displays an example of

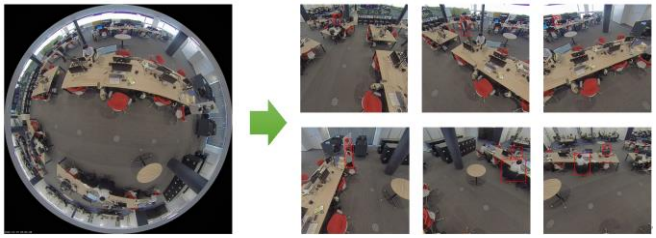

Fig. 3 Expansion of fish-eye image and example of AI inference

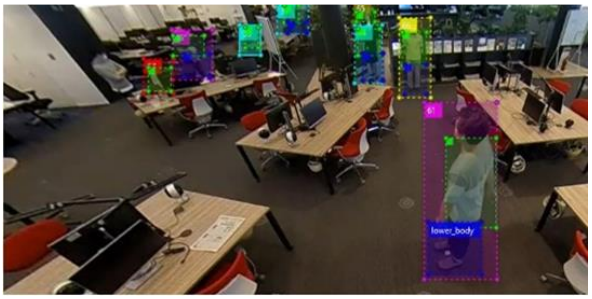

Fig. 4 Example of training data

Fig. 5 Results of pose estimation
(Person feature point detection)

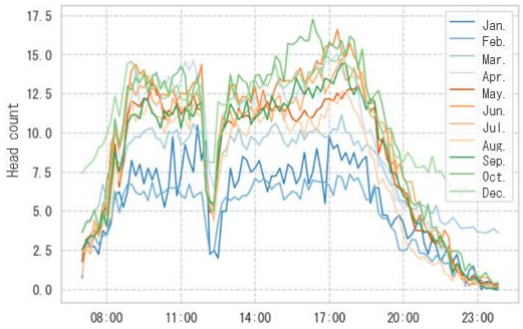

Fig. 6 Time-series changes in the number of occupants for each month

Fig. 7 Heat map of occupants

the pose estimation results. By estimating states such as standing and sitting, more detailed information about building users can be obtained.

Fig. 6 depicts the time-series changes in the number of occupants during the evaluation period was from December 1, 2020 to October 31, 2021. It can be observed from the figure that the number of people counted were small from January to March. This coincides with the period (January 8 to March 21, 2021) during which Chiba Prefecture, where the Takenaka Research and Development Institute is located, declared a state of emergency owing to the spread of COVID-19 and implemented measures such as working from home instead of commuting to the office. Additionally, a drop in the number of people counted at around 12:00 in each month was observed, which was attributed to building users leaving their desks for a lunch break. However, multiple people were detected at night, which did not match the actual usage of the building. After checking the camera images, it was found that the accuracy of the image analysis decreased because the building lights were turned off after 19:00, resulting in an increased number of false positives. Fig. 7 illustrates the results of a heat map display of the estimated locations of building users in October, when the number of people counted was particularly high. It can be observed that the position estimation results were concentrated around seats. Additionally, as a countermeasure against the spread of COVID-19, the seating positions in the building were set up diagonally. It was confirmed that the building users were seated diagonally and that the position estimation results were accurate.

A dataset similar to the one described above was created to estimate the insulation value. A fine-tuned model was used with DenseNet201[5] as the base model, and it was trained to estimate 19 clothing patterns (insulation values) typically found in office environments. Fig. 8 shows the correct response rate for the test data (573 types). The average correct response rate was 77%, although the rate tended to decrease when the number of training images was small. In this study, only the upper body was subject to estimation, and the whole body insulation value (clo value) was obtained by adding the lower body as a fixed value. This is because it is difficult to separate the upper and lower bodies with the current algorithm. However, because the clo value for the lower body is almost constant in office environments, it is considered valid.

Category	Long-sleeve shirt	Short-sleeve shirt	Long-sleeve T-shirt	Short-sleeve T-shirt	Sleeveless shirt	Long-sleeve shirtdress
Training (number of images)	1224	1109	298	938	61	85
Test (number of images)	115	120	25	98	4	3
Accuracy (%)	80.87	76.67	64.00	78.57	50.00	100.00

Category	Short-sleeve shirtdress	Sleeveless vest	Long-sleeve sweater	Long-sleeve sweat shirt	Long-sleeve cardigan	Turtle-neck sweater
Training (number of images)	70	68	273	146	178	34
Test (number of images)	10	3	29	15	12	4
Accuracy (%)	90.00	33.33	79.31	46.67	41.67	50.00

Category	Jacket	Long coat	Short coat	Short coat	Windbreaker jacket	Down jacket
Training (number of images)	718	219	135	91	4	169
Test (number of images)	73	19	18	3	2	20
Accuracy (%)	87.67	78.94	66.67	100.00	0.00	95.00

	Total
Training (number of images)	5820
Test (number of images)	573
Accuracy (%)	77.49

Blue : Accuracy > 50%
Red : Accuracy <= 50%

Fig. 8 Accuracy of the clothing insulation value estimation model

4 Development of equipment control method using deep learning

4.1 Application to optical environment control and verification of effect

In the target building[2], a luminance control system was used to control lighting, blinds, and louvers to reduce lighting power consumption during daylight. As shown in Fig. 9, luminance cameras are installed in various places in the room. The average luminance of a predetermined area (window surface, wall surface, floor surface, etc.) is calculated from the captured image, and each device is controlled so that the average luminance falls within the target luminance range determined for each area. This control is referred to as “local control” for convenience. Local control systems establish rules for controlling the order of operation for devices in each area when the target luminance range is exceeded. If the luminance remains outside the target range after operating the blinds or louvers, the lighting dimming rate is adjusted. However, in this research and development, reinforcement learning methods are utilized to create a model that learns from past data, determines the behavior that maintains indoor luminance within the target range while minimizing power consumption, and controls each device. This approach is referred to as AI control. Table 1 provides a summary of the input/output data that are utilized for AI control model learning.

Fig. 10 shows an overview of the AI control model. This model is constructed by combining two models. The first is a predictive AI model that predicts indoor luminance based on accumulated past operational data, allowing for the simulation of luminance by various devices under certain conditions. The predictive AI model used LightGBM[6], which is a decision tree-based algorithm. Additionally, past data was utilized to learn the relationship between device operation status (state/behavior), power consumption, and rewards determined from luminance, as shown in Table 1. The second model is a reinforcement learning AI model that selects the optimal method of operating equipment. The reinforcement learning AI model used DDPG[7], which is a reinforcement learning method that is positioned between the actor-critic policy gradient method and Q-learning. These models were built during the learning period of June to November 2020, and put into operation in the real environment from January 2021. However, a gap in the data existed because most of the operating data used in the initial model were for local control, which controls

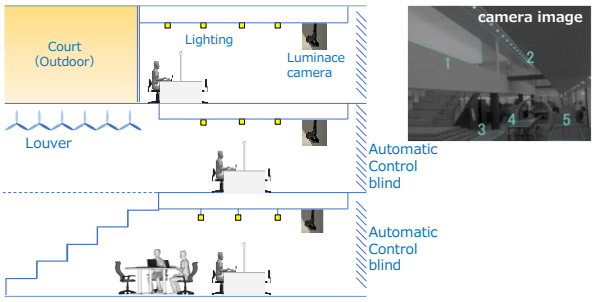

Fig. 9 Light environment control based on brightness

Table 1 Input / output and reward of AI model for light environment control

Objective	(1) Average luminance of each area must be within the target luminance range (2) Minimize lighting power consumption
Input data	Sun altitude/azimuth angle, solar radiation, atmospheric pressure dimming rate, louver angle, blind angle/height
Action (Operation target)	(1) Light dimming rate (2) Louver angle (3) Blind angle (4) Blind height 136 point
Reward function	rewards = - Σ (Lighting power consumption*1 + weight α × penalties*2) *1···Rated power × number of lights × dimming ratio × coefficient *2···Rated power × number of lights(Luminaires operating in an area when luminance is out of the target luminance range)
Training data period	Jun., 2020 ~ May, 2021 (The first model was built by training using data obtained between Jun., 2020 and Nov., 2020, and the model was updated by re-training in May 2021.)

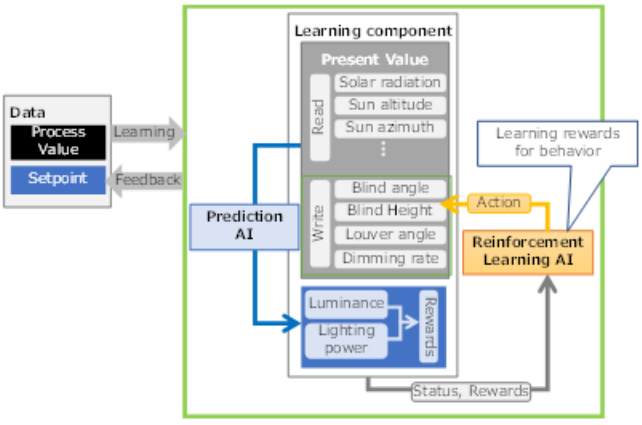

Fig. 10 Overview of AI model for light environment control

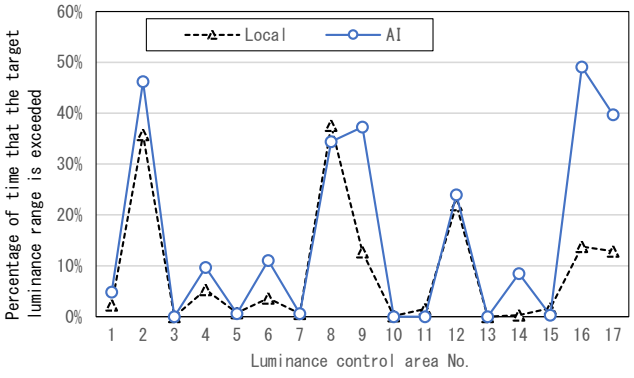

Fig. 11 Comparison of BAS and AI system with respect to brightness control

equipment based on rules. Therefore, in May 2021, the training data were expanded to one year (June 2020 to May 2021), and re-learning was conducted to update the AI model.

We assessed the effectiveness of the control system by examining the indoor luminance control performance. Fig. 11 illustrates the percentage of time the luminance was outside the target range under both the local and AI control methods. While the effectiveness of both methods varied based on the control area, areas that exhibited poor controllability with local control tended to perform worse with AI control as well. In certain areas, AI control deviated from the target luminance range for a longer time than local control. Specifically, areas exposed to solar radiation, such as those located under skylights and near windows, were more susceptible to deviations from the target luminance range. In this study, the penalty weighting factor in the reward calculation was the same for all areas. However, we believe that adjusting the weighting factor for each area may improve the system's performance.

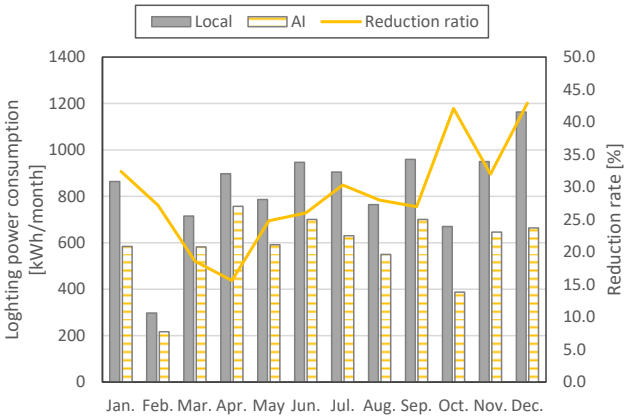

Fig. 12 Energy saving effect by AI control system

Fig. 12 displays the comparison between the lighting power consumption under AI control and local control for the period of January to December 2021. The AI control lighting power consumption is based on actual measured values, while the local control result is the sum of selected days when the amount of solar radiation was almost identical. Despite potential weather-related variations, a reduction in power consumption of 15-40% was observed for each month. Furthermore, the annual lighting power consumption was found to be reduced by approximately 29%.

4.2 Application to air conditioning control and effect verification

For air conditioning control, in this development, we constructed an AI-based control system for (1) improving the air conditioning start time and (2) optimizing the heat source water supply temperature.

(1) Improvement of air conditioning start time and effect verification

The time required for the room temperature to rise to the optimum temperature (set temperature or control temperature) from the air conditioning start time varies depending on factors, such as weather conditions, indoor load conditions, and hot/cold water temperatures; thus, it is possible to conserve energy by adjusting the air conditioning start time according to the cooling/heating load (see Fig. 13). Many buildings often have fixed start times to accommodate scheduled operations, but this can result in wasted air conditioning time if the temperature reaches the desired level earlier than the work start time. However, the air conditioning energy consumption can be reduced by appropriately adjusting the air conditioning start time based on the outside air temperature, room temperature, and operating conditions of the heat source and air conditioner. In this study, we developed an AI model that predicts the optimum air conditioning start time that can achieve the appropriate temperature by the work start time and also conserve energy based on various data collected in the data platform. We then verified the effectiveness of the model.

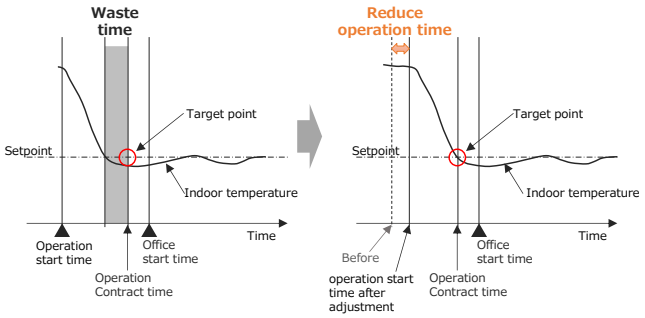

Fig. 13 Improvement of air conditioning start time

Table 2 presents the input and output data used for the AI model. In the target building, the air conditioning was scheduled to start at 6:00 every day, and the room temperature was adjusted to the appropriate temperature by 8:30 during working hours. The objective of the developed system was to automatically adjust the air conditioning start time so that the room temperature reaches the appropriate temperature at 8:00, which is 30 minutes before the end of working hours. The constructed AI model predicts the average temperature of each floor at 8:00 using features such as outside air temperature, indoor temperature and humidity, heat supply amount, and air conditioning operation status. The room temperature was predicted every 10 minutes from 6:00 to 8:00,

and if the temperature exceeded the optimal temperature during cooling, a command was sent to the automatic control via the data platform to start the air conditioning operation. Separate models need to be created for cooling and heating because the prediction model exhibits varying room temperature behavior for each. However, in the demonstration building, the rooms were open from the first to the third floors, and it takes time for the room temperature to rise to the appropriate level during heating. Thus, delaying the air conditioning start time has no effect on the heating results. The cooling results are described below.

Table 2 Input / output of AI model for air conditioning start time

Objective	Reduction of wasted operating time
Input data	Outdoor temperature/humidity, solar radiation, rain, sunset, Chilled/hot water load/on/off for each HVAC device, supply water temperature, average temperature/huidity of each floor, time, holiday
Model	LightGBM
Prediction target	Indoor temperature at 8:00 a.m. when air conditioning is not in operation *Judges whether the set point (cooling: 26°C, heating: 22°C) is reached or not.
Operation target	On/Off of each HVAC device
Training data period	Jun., 2020 ~ Oct., 2020

Fig. 14 shows the results of comparing the predicted values of the AI model and the measured values. The legend in the figure indicates the predicted time, and it can be observed that the room temperature at 8:00 could be predicted with good accuracy within ±0.5 °C, regardless of the predicted time.

Fig. 15 shows an example of the time-series changes in air conditioning start time delayed by AI control and normal control, which starts the air conditioning at 6:00. In both types of control, power consumption fluctuates significantly when air condition is started because of the large load caused by the water temperature in the pipes and indoor conditions. However, it can be observed that the fluctuation gradually changed after approximately 1 h from the start. Therefore, to calculate the energy-conserving effect achieved by delaying the air conditioning start time, we used the following formula:

Air conditioning power reduction due to air conditioning start delay (kWh)

= Power consumption 1–2 h after starting air conditioning (kWh/h) × delay time (h)

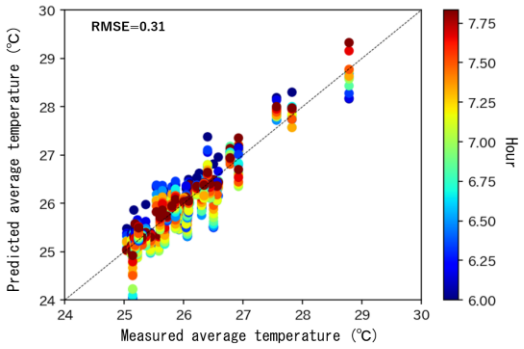

Fig. 14 Comparison of room temperature predicted value and actual value

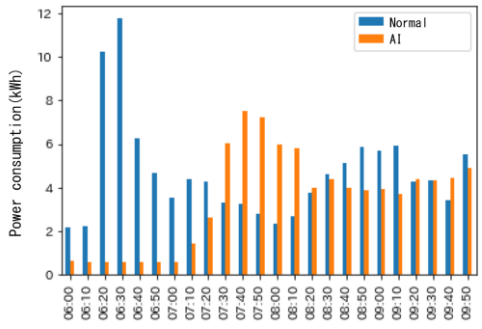

Fig. 15 Changes in air conditioning power consumption when the air conditioning start time is adjusted

Fig. 16 shows the results of a trial calculation of the annual energy conservation effect achieved by optimizing the air conditioning start time. The power consumption during AI control is the actual value, and the power consumption of the normal control is the value obtained by adding the amount of air conditioning power reduction during AI control to the actual value calculated using the formula described above. It can be observed that the reduction rate in the intermediate period is significant, and there was a reduction effect of approximately 20–30% for the air conditioning power consumption from 6:00 to 9:00. Additionally, there was a reduction effect of approximately 2–5% even in the summer. This reduction was approximately 1.8% of the air conditioning power consumption during the entire cooling period.

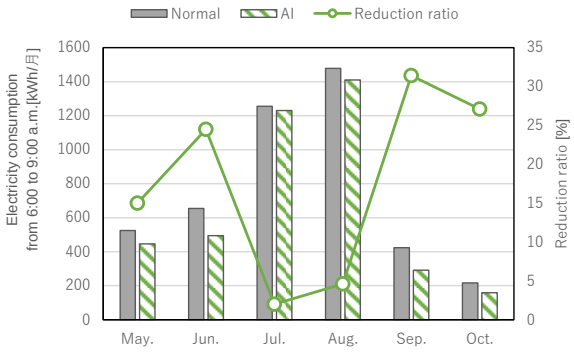

Fig. 16 Energy saving effect by optimizing the air conditioning start timez

(2) Optimization of heat source water supply temperature

Fig. 17 shows the relationship between the heat source system COP and water supply temperature. COP is defined as the amount of cold/hot water heat generated by the heat source/power consumption of the heat source system (including pump power) and is an indicator of heat source efficiency. Taking cooling as an example, the COP of the heat source system increases as the water supply temperature increases, indicating that the system operates with high efficiency (i.e., energy is being conserved). However, if the water supply temperature is raised too high, the room cannot be cooled or dehumidified, and the indoor environment deteriorates. Therefore, in the AI model design, rewards and constraints were set to maintain the room temperature and humidity of each room in the target area while minimizing the power consumption of the heat source system.

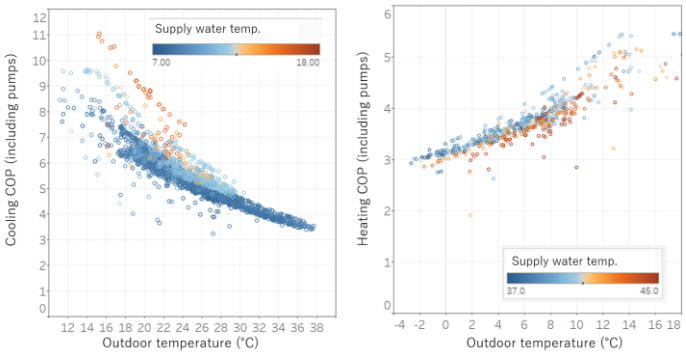

Fig. 17 Relationship between COP of HVAC system and water supply temperature (left : during cooling, right : during heating)

Table 3 shows the organized input and output data of the AI model. In this model, the difference between the set temperature and the actual room temperature of multiple rooms is set as a penalty, and the reward is the sum of the penalty multiplied by a weight and the power consumption of the heat source system multiplied by -1. As with the light environment control, LightGBM was used to perform supervised learning and build a model to predict this reward. Additionally, the method of determining the water supply temperature entailed using this prediction model to predict the rewards when multiple water supply temperatures were selected. We selected the water supply temperature that maximized the reward. In cases where the predicted rewards were the same, the median value of those water supply temperatures was selected. When implementing the control in this model, the control interval was set to 30 min, and the effect was verified for the air conditioning operating hours from 6:00 to 18:00. Although predictions were made to maximize the reward, in cases where the indoor environment deteriorated (e.g., room temperature deviating from set temperature, ineffective dehumidification), then the rule of forcibly returning the water supply temperature was applied to maintain the comfort of the indoor environment.

Table 3 Input / output and reward of AI model for water supply temperature

Objective	(1) Indoor temperature must be within ±2°C of the set temperature. (2) Minimize heat source power consumption
Input data	Outdoor temperature/humidity, solar radiation, rain, sunset, Chilled/hot water load, indoor temperature/humidity, setpoint for each HVAC device
Action (Operation target)	Chilled and hot water supply temperature
Reward function	Rewards = - Σ (Power consumption (of heatsource equipment) *1 + weight α × penalties*2) *1…Since the target area is part of the entire building, the load of each HVAC device was summed and the power consumption was calculated using the power consumption characteristic equation created from the measured data. *2…Difference between setpoint and actual indoor temperature
Training data period	Cooling…Jun., 2020 ~ Sep., 2020 Heating…Nov., 2020 ~ Dec., 2020

This was operated in the demonstration building for one year to understand the annual energy-conserving effect of AI control. Fig. 18 shows the results of a comparison of the power consumption of the heat source system under AI control and normal control. Here, the power consumption of AI control is an actual value, but the power consumption of normal control is a calculated value. Specifically, the calculations were made on the assumption that cold water was kept at 7 °C during cooling and hot water at 45 °C during heating when processing the same heat load as under AI control, based on the relationship between the water supply temperature and the heat source system COP obtained from past operation data and pump efficiency.

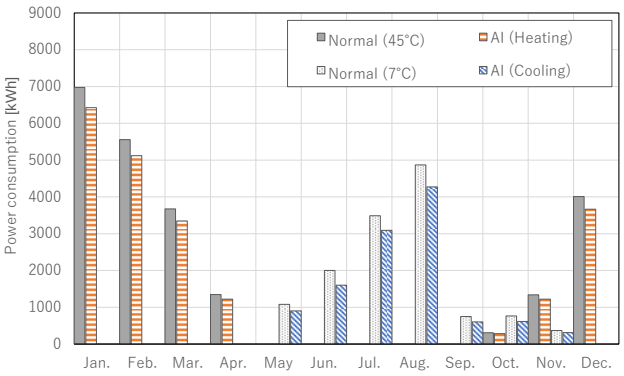

Fig. 18 Energy saving effect by AI control system

The figure shows that AI control achieved energy-conserving operations, with reduction rates of 14.4% during the cooling period and 8.1% during the heating period,

resulting in a reduction of 10.6% of the annual heat source power consumption. The energy-conserving effect during the cooling period includes the improvement in the air conditioning start time, as described in the previous section. The reduction rate during heating is smaller than that during cooling, which is attributed to the characteristics of the target heat source equipment. This is because, as can be observed from the relationship between the heat source system COP characteristic and the water supply temperature, the COP improvement effect due to changes in the water supply temperature was smaller during heating than during cooling.

5 Summary

To realize smart buildings, we developed a data linkage platform that centralizes information. Furthermore, we utilized technologies to obtain user information and implement equipment control technologies that minimize energy consumption while maintaining comfort in offices that are actually in operation. The data collected over a period of more than a year was then analyzed and verified.

To extract human factors, we created a dataset of insulation value that are typically found in office settings, which was previously unavailable. We then built a system that can estimate a person's position, pose, and insulation value while keeping development costs low by fine-tuning a pre-trained model. In the future, this user information can be used to develop applications for equipment interlocking control and space usage analysis. Furthermore, for building facility control using AI, we developed a facility control system that uses machine learning based on operational data obtained from a data platform. After operating the system for one year, we confirmed that we were able to establish control that achieved both energy conservation and an indoor environment.

Acknowledgements

The results of this research were obtained as a result of a subsidized project by the New Energy Industrial Technology Development Organization (NEDO).

References

1) Kasuya, T. et al.: "futaba: Bigdata platform for smart building", Journal of the Information Processing Society of Japan, Vol. 62, No. 3, p. 867-876, 2021

2) Higuchi, Y. et al.: "Special feature: Takenaka Research and Development Institute Renewal Project–Planning and evaluation of renewal of research facilities in consideration of human diversity", Takenaka Technical Research Report No. 76, December 2020

3) https://supervise.ly/explore/models/ssd-inception-v-2-coco-1861/overview

4) https://docs.openvino.ai/2020.3/_models_intel_human_pose_estimation_0001_description_human_pose_estimation_0001.html

5) G.Huang, et al：Densely Connected Convolutional Networks. IEEE Conference on Pattern Recognition and Computer Vision (CVPR), 2016.

6) Guolin Ke, et al.：LightGBM: A highly efficient gradient boosting decision tree. In Advances in Neural Information Processing Systems, pages 3149-3157, 2017.

7) David Silver, et al：Deterministic policy gradient algorithms, in Proc. of the 31st ICML, Vol.32, pp.387-395, 2014